ELSEVIER

Available online at www.sciencedirect.com
SCIENCE DIRECT®
Inorganica Chimica Acta 358 (2005) 2575–2584

Inorganica Chimica Acta
www.elsevier.com/locate/ica

Influence of the phosphine arrangement on the reactivity of palladium(II) and platinum(II) polyphosphine complexes with copper(I) chloride

Damián Fernández, M. Inés García-Seijo, Paloma Sevillano, Alfonso Castiñeiras, M. Esther García-Fernández *

Department of Inorganic Chemistry, University of Santiago de Compostela, Avda. de las Ciencias s/n, E-15782 Santiago de Compostela, Spain

Received 5 February 2004; accepted 6 March 2005
Available online 6 April 2005

Abstract

The distorted square-planar complexes [Pd(PNHP)Cl]Cl (**1**) (PNHP = bis[2-(diphenylphosphino)ethyl]amine), [M(P_3)Cl]Cl [P_3 = bis[2-(diphenylphosphino)ethyl]phenylphosphine; M = Pd (**2**), Pt (**3**)] and [Pt(NP_3)Cl]Cl (**5**) (NP_3 = tris[2-(diphenylphosphino)ethyl]amine), coexisting in the later case with a square-pyramidal arrangement, react with one equivalent of CuCl to give the mononuclear heteroionic systems [M(L)Cl]($CuCl_2$) [L = PNHP, M = Pd (**1a**); L = P_3, M = Pd (**2a**), Pt (**3a**); L = NP_3, M = Pt (**5a**)]. The crystal structure of **3a** confirms that Pt(II) retains the distorted square-planar geometry of **3** in the cation with P_3 acting as tridentate chelating ligand, the central P atom being *trans* to one chloride. The counter anion is a nearly linear dichlorocuprate(I) ion. However, the five-coordinate complexes [Pd(NP_3)Cl]Cl (**4**), [M(PP_3)Cl]Cl (M = Pd (**6**), Pt (**7**); PP_3 = tris[2-(diphenylphosphino)ethyl] phosphine) containing three fused five-membered chelate rings undergo a ring-opening by interaction with one (**4**, **6**, **7**) and two (**6**, **7**) equivalents of CuCl with formation of neutral MCu(L)Cl_3 [L = NP_3, M = Pd (**4a**); L = PP_3, M = Pd (**6a**), Pt (**7a**)] and ionic [MCu(PP_3)Cl_2]($CuCl_2$) [M = Pd (**6b**), Pt (**7b**)] compounds, respectively. The heteronuclear systems were shown by ^{31}P NMR to have structures where the phosphines are acting as tridentate chelating ligands to M(II) and monodentate bridging to Cu(I). Further additions of CuCl to the neutral species **6a** and **7a** in a 1:1 ratio resulted in the achievement of the ionic complexes **6b** and **7b** with $CuCl_2^-$ ions as counter anions. It was demonstrated that the formation of heterobimetallic or just mononuclear mixed salt complexes was clearly influenced by the polyphosphine arrangement with the tripodal ligands giving the former compounds. However, complexes [M(NP_3)Cl]Cl constitute one exception and the type of reaction undergone versus CuCl is a function of the d^8 metal centre.

Keywords: Pd(II) and Pt(II) complexes; Linear and tripodal polyphosphines; Reactions with CuCl; Heteronuclear systems; ^{31}PNMR spectroscopy; Crystallography of a dichlorocuprate(I)

---

1. Introduction

Homo- and heterobinuclear complexes containing bridged and heterobridged halide, sulfide, dithiolato, alkynyl, diphosphine, aminophosphine and other hybrid ligands were shown to play a prominent role as starting materials in organometallic chemistry providing the

---

* Corresponding author. Tel.: +34 981 563100/14241; fax: +34 981 597525.
E-mail address: qiegfq@usc.es (M.E. García-Fernández).

0020-1693/$ - see front matter © 2005 Elsevier B.V. All rights reserved.
doi:10.1016/j.ica.2005.03.018

means for the study of cooperative bimetallic reactivity and the achievement of materials with novel structures and desirable properties [1–8]. Thus, the heterobimetallic chloride-bridged d^{6-8} complexes $[(PEt_3)(\eta^5\text{-}C_5Me_5)M'(\mu\text{-}Cl)_2Pt(C_6F_5)_2]$ (M′ = Rh, Ir) react with the alkynylating agents $[M''(C{\equiv}CR)]_n$ (M″ = Cu, Ag) with formation of novel heterotetrametallic d^6–d^{10}–d^8 polyalkynyl compounds $[(PEt_3)Cp^*M'(\mu\text{-}1kC^{\alpha}{:}\eta^2\text{-}C{\equiv}CPh)_2M''_2(\mu\text{-}4kC^{\alpha}{:}\eta^2\text{-}C{\equiv}CPh)_2Pt(C_6F_5)_2]$, in which two widely divergent bis(alkynyl)metal fragments (d^6 and d^8) are connected through d^{10} (Cu or Ag) metal ions [4b]. However, similar reactions between [*cis*-$M(C_6F_5)_2(thf)_2$] (M = Pd, Pt) and $[\{M'Cp^*Cl(\mu\text{-}Cl)\}_2]$ (M′ = Rh, Ir) involve a chloride transfer to yield the mixed salt complexes $\{Cp^*M'(\mu\text{-}Cl)_3M'Cp^*\}_2[\{(C_6F_5)_2M(\mu\text{-}Cl)\}_2]$. On the other hand, the heterometallic sulfide clusters $[Cu_4(dcpm)_4(M^{\#}S_4)](ClO_4)_2$ containing a bulky phosphine ligand (dcpm = bis(dicyclohexylphosphino)methane) and obtained by reaction of $[Cu_2(dcpm)_2(MeCN)_2](ClO_4)_2$ with $M^{\#}S_4{}^{2-}$ ($M^{\#}$ = Mo, W) are luminescent systems with a saddle shaped $\{Cu_4M^{\#}S_4\}$ core and unusual $\{Cu_4P_8Cu_4\}$ metallomacrocycles [9]. Although bimetallic combinations with diphosphine assembling ligands are relatively common [5,8d,10], little work has been directed towards the study of heteronuclear compounds containing triphosphine or tetraphosphine ligands. One of these reports describes the reaction of *syn*-$[Pt_2(\mu\text{-}dpmp)_2(xylNC)_2](PF_6)_2$ (dpmp = bis(diphenylphosphinomethyl)phenylphosphine) with CuX (X = Cl, Br, I) to give the heterotrinuclear complex $[Pt_2CuX(\mu\text{-}dppm)_2(xylNC)_2](PF_6)_2$ with a rhombic Pt_2CuX structure. In contrast, the same reaction with CuI in the presence of NH_4PF_6 or with $[Cu(CH_3CN)_4](PF_6)$ gives a diplatinum (II) compound, $[Pt_2(\mu\text{-}dpmp)_2\text{-}(xylNC)](PF_6)_2$, that could be regarded as a product derived from removal of one isocyanide molecule from the precursor with the subsequent ring-closure process since the preexistent dangling phosphorus atom coordinates now to Pt(II) [11].

In previous works, we demonstrated that the square-planar complexes $[M(P_3)X]X$ (M = Pd, Pt; P_3 = bis[2-(diphenylphosphino)ethyl]phenylphosphine; X = Cl, Br, I) undergo a ring-opening reaction upon addition of Au(I) to give the heterobimetallic compounds $MAu(P_3)X_3$ [M = Pd, X = Cl, Br, I; M = Pt, X = Cl, Br] containing distorted square-planar M(II) and linear Au(I) centres [12,13]. However, the reaction with AgCl does not take place and with $AgNO_3$ affords the nitrate derivatives $[M(P_3)(ONO_2)](NO_3)$ [13]. The study of similar reactions with Au(I) or Ag(I) for complexes containing tripodal polyphosphines such as $[Pd(NP_3)X]X$ (NP_3 = tris[2-(diphenylphosphino)ethyl]amine) or $[M(PP_3)X]X$ (PP_3 = tris[2-(diphenylphosphino)ethyl] phosphine) (X = Cl, Br, I) is very scarce [14,15] and less work has been done to investigate reactions between Cu(I) and metal–polyphosphine complexes [14]. This prompted us to be interested in using precursors containing linear or tripodal polyphosphines such as [M(L)Cl]Cl (M = Pd, Pt; L = PNHP = bis[2-(diphenylphosphino)ethyl]amine, P_3, NP_3, PP_3), for reactions with CuCl. The polyphosphine arrangement resulted to be decisive in the formation of either mononuclear heteroionic or heterodinuclear systems, the linear ligands affording only the former ones.

2. Experimental

2.1. General procedures and instrumentation

Palladium chloride and potassium tetrachloroplatinate were purchased from Strem Chemicals, copper chloride, tris[2-(diphenylphosphino)ethyl]phosphine and bis[2-(diphenylphosphinoethyl)]phenylphosphine from Aldrich, sodium chloride from Panreac. Microanalyses were performed on a Fisons Instrument EA 1108 CHNS-O. Fast atom bombardment (FAB) or liquid secondary-ion (L-SIMS) mass spectra were obtained in a Micromass Autospec spectrometer using nitrobenzylic alcohol as the matrix. Infrared spectra were recorded at ambient temperature as KBr pellets (4000–500 cm^{-1}) and Nujol mulls (500–100 cm^{-1}) on a Mattson Cygnus 100 spectrophotometer. The bands are reported as vs = very strong, s = strong, m = medium, w = weak, sh = shoulder, br = broad. $^{31}P\ \{^1H\}$ and $^{195}Pt\ \{^1H\}$ NMR spectra were recorded on a Bruker AMX500 spectrometer at 202.46 and 107.52 MHz, respectively. Chemical shifts (δ) are reported in ppm relative to external 85% H_3PO_4 (^{31}P) and 1 M Na_2PtCl_6 (^{195}Pt); s = singlet, d = doublet, t = triplet, dt = doublet of triplets, dq = doublet of quartets, br = broad signal, J = coupling constant in Hz. Conductivities were measured at 25 °C using 10^{-3} M solutions in DMF or CH_3CN on a WTW model LF-3 instrument.

2.2. Syntheses

2.2.1. Aminophosphines

NP_3 and PNHP were prepared following the procedures previously described [16,17].

2.2.2. Syntheses of **1**–**7**

A solution of PNHP (1.0471 mmol), P_3 (1.1220–1.8700 mmol), NP_3 (0.4594–0.6125 mmol) in CH_2Cl_2 (8–50 ml) or PP_3 (0.2922–0.4160 mmol) in $CHCl_3$ (25–35 ml) was added dropwise to a solution of Na_2PdCl_4 [17] in MeOH (12 ml, **4**) or H_2O (15–25 ml, **1**, **2**, **6**) or to a solution of K_2PtCl_4 in H_2O (15–35 ml, **3**, **5**, **7**) in 1:1 stoichiometric ratio. The resultant mixtures were stirred for 1–24 h at room temperature and after that solvents were partially removed in vacuo to leave a solution (**4**) that was filtered or a suspension (**1**–**3**, **5**–**7**). Et_2O was added to complete the precipitation and solids were filtered off, washed with H_2O and dried in vacuo. Complexes **1**–**3** and **5** were recrystallised from CH_2Cl_2/*n*-hexane (**1**–**3**) or MeOH/*n*-hexane (**5**) and then dried in vacuo. **1** · H_2O: Yield: 90%, white solid, m.p. 172 °C. $C_{28}H_{31}NP_2PdCl_2O$ requires: C, 52.7; H, 4.9; N, 2.3. Found: C, 52.4; H, 4.8; N, 2.2%. IR ν_{max}/cm^{-1} 3436s (N–H); 312s (Pd–Cl). MS (FAB): *m*/*z* 582 ($M^+ - Cl$, 100%); 547 ($M^+ - 2Cl$, 8%). Λ(DMF) = 22.8 $ohm^{-1}\,cm^2\,mol^{-1}$. (**2**): Yield: 68%, white solid, m.p. 210 °C. $C_{34}H_{33}P_3PdCl_2$ requires: C, 57.3; H, 4.7. Found: C, 57.0; H, 4.9%. IR ν_{max}/cm^{-1} 318vs (Pd–Cl). MS (FAB): *m*/*z* 675 ($M^+ - Cl$, 100%). Λ(DMF) = 91.5 $ohm^{-1}\,cm^2\,mol^{-1}$. (**3**): Yield: >70%, white solid, m.p. > 250 °C. $C_{34}H_{33}P_3PtCl_2$ requires: C, 51.0; H, 4.1. Found: C, 51.2; H, 4.3%. IR ν_{max}/cm^{-1} 320vs (Pt–Cl). MS (FAB): *m*/*z* 764 ($M^+ - Cl$, 100%). Λ(DMF) = 82.9 $ohm^{-1}\,cm^2\,mol^{-1}$. (**4**) · $2H_2O$: Yield: 70%, orange solid, m.p. 161 °C (dec.). $C_{42}H_{46}NP_3PdCl_2O_2$ requires: C, 58.1; H, 5.4; N, 1.6. Found: C, 58.1; H, 5.8; N, 1.6%. IR ν_{max}/cm^{-1} 300w (Pd–Cl). MS (FAB): *m*/*z* 794 ($M^+ - Cl$, 17%). $\Lambda(CH_3CN)$ = 139.2 $ohm^{-1}\,cm^2\,mol^{-1}$. (**5**) · $4H_2O$: Yield: 63%, orange solid, mp > 250 °C. $C_{42}H_{50}NP_3PtCl_2O_4$ requires: C, 50.8; H, 5.1; N, 1.4. Found: C, 50.1; H, 5.4; N, 1.4%. IR ν_{max}/cm^{-1} 305sh (Pt-Cl). MS (FAB): *m*/*z* 883 ($M^+ - Cl$, 4%); 848 ($M^+ - 2Cl$, 3%). Λ(DMF) = 39.8 $ohm^{-1}\,cm^2\,mol^{-1}$. (**6**) · $4H_2O$: Yield: 92%, red solid, m.p. 260 °C. $C_{42}H_{50}P_4PdCl_2O_4$ requires: C, 55.6; H, 5.6. Found: C, 55.0; H, 5.4%. IR ν_{max}/cm^{-1} 284s (Pd–Cl). MS (L-SIMS): *m*/*z* 811 ($M^+ - Cl$, 56%); 776 ($M^+ - 2Cl$, 2%). Λ(DMF) = 77.1 $ohm^{-1}\,cm^2\,mol^{-1}$. (**7**) · $2H_2O$: Yield: 85%, yellow solid, m.p. 281 °C. $C_{42}H_{46}P_4PtCl_2O_2$ requires: C, 51.8; H, 4.7. Found: C, 51.4; H, 4.7%. IR ν_{max}/cm^{-1} 275s (Pt–Cl). MS (L-SIMS): *m*/*z* 900 ($M^+ -$ Cl, 45%); 865 ($M^+ - 2Cl$, 1%). Λ(DMF) = 72.1 $ohm^{-1}\,cm^2\,mol^{-1}$.

2.2.3. *Syntheses of **1a**–**7a** and **6b**–**7b***

To a solution of **1** · H_2O (0.1886 mmol) in CH_2Cl_2 (20 ml), **2**, **3**, (**6**) · $4H_2O$ and (**7**) · $2H_2O$ (0.1250–0.2273 mmol) in $CHCl_3$ (15–40 ml), **4** · H_2O and (**5**) · $4H_2O$ (0.1512–0.1731 mmol) in MeOH (15–20 ml), CuCl was added, as a solid, in the appropriate stoichiometric ratio. The resultant mixtures were stirred for 0.5–24 h at room temperature and after that Et_2O (**1**, **4**–**7**) or *n*-hexane (**2**, **3**) was added to precipitate the solids. The complexes were filtered off and dried in vacuo. Crystals of **3a**, suitable for X-ray diffraction, were obtained by recrystallisation from acetone/Et_2O. (**1a**) · H_2O: Yield: 45%, green solid, m.p. 150 °C (dec.). $C_{28}H_{31}NP_2PdCuCl_3O$ requires: C, 45.6; H, 4.3; N, 1.9. Found: C, 45.1; H, 4.3; N, 1.8%. IR ν_{max}/cm^{-1} 3446m, br (N–H); 314s (Pd–Cl); 396m ν_a(Cu–Cl); 296w ν_s(Cu–Cl).IR δ/cm^{-1} 109sh ($CuCl_2$). MS (FAB): *m*/*z* 582 ($M^+ - Cu - 2Cl$, 34%). $\Lambda(CH_3CN)$ = 67.1 $ohm^{-1}\,cm^2\,mol^{-1}$. **2a**: Yield: 90%, yellow solid, m.p. 233 °C. $C_{34}H_{33}P_3PdCuCl_3$ requires: C, 50.3; H, 4.1. Found: C, 49.1; H, 3.9%. IR ν_{max}/cm^{-1} 317vs (Pd–Cl); 404s ν_a(Cu–Cl); 282m ν_s(Cu–Cl). IR δ/cm^{-1} 115s ($CuCl_2$). MS (FAB): *m*/*z* 675 ($M^+ - Cu - 2Cl$, 98%). Λ(DMF) = 80.8 $ohm^{-1}\,cm^2\,mol^{-1}$. **3a**: Yield: 79%, yellow solid, m.p. > 250 °C. $C_{34}H_{33}P_3PtCuCl_3$ requires: C, 45.4; H, 3.7. Found: C, 44.9; H, 3.6%. IR ν_{max}/cm^{-1} 320vs (Pt–Cl); 400s ν_a(Cu–Cl); 282m ν_s(Cu–Cl). IR δ/cm^{-1} 117s ($CuCl_2$). MS (FAB): *m*/*z* 765 ($M^+ - CuCl_2$, 100%). Λ(DMF) = 82.9 $ohm^{-1}\,cm^2\,mol^{-1}$. (**4a**) · $2H_2O$: Yield: 70%, yellow solid, m.p. 250 °C (dec.). $C_{42}H_{46}NP_3PdCuCl_3O_2$ requires: C, 52.2; H, 4.8; N, 1.4. Found: C, 52.1; H, 4.8; N, 1.1%. IR ν_{max}/cm^{-1} 337m (Pd–Cl); 255w (Cu–Cl). MS (FAB): *m*/*z* 892 ($M^+ - Cl$, 3%); 794 ($M^+ - Cu - 2Cl$, 7%); 759 ($M^+ - Cu - 3Cl$, 1%). $\Lambda(CH_3CN)$ = 35.6 $ohm^{-1}\,cm^2\,mol^{-1}$. (**5a**) · $4H_2O$: Yield: 73%, green solid, m.p. 205 °C. $C_{42}H_{50}NP_3PtCuCl_3O_4$ requires: C, 46.3; H, 4.6; N, 1.3. Found: C, 46.4; H, 5.2; N, 1.3%. IR ν_{max}/cm^{-1} 290s (Pt–Cl); 390vs ν_a(Cu–Cl); 290vs ν_s(Cu–Cl). IR δ/cm^{-1} 115sh ($CuCl_2$). MS (FAB): *m*/*z* 884 ($M^+ - Cu - 2Cl$, 55%); 848 ($M^+ - Cu - 3Cl$, 11%). Λ(DMF) = 54.7 $ohm^{-1}\,cm^2\,mol^{-1}$. (**6a**) · $2H_2O$: Yield: 90%, brown solid, m.p. 180 °C. $C_{42}H_{46}P_4PdCuCl_3O_2$ requires: C, 51.3; H, 4.7. Found: C, 51.8; H, 4.8%. IR ν_{max}/cm^{-1} 300vs, br (Pd–Cl); 285vs (Cu–Cl). MS (L-SIMS): *m*/*z* 909 ($M^+ - 2Cl$, 5%); 874 ($M^+ - 3Cl$, 1%) 811 ($M^+ - Cu - 2Cl$, 56%). Λ(DMF) = 23.2 $ohm^{-1}\,cm^2\,mol^{-1}$. (**7a**) · $4H_2O$ · Et_2O: Yield: 85%, yellow solid, m.p. 182 °C. $C_{46}H_{60}P_4PtCuCl_3O_5$ requires: C, 46.7; H, 5.1. Found: C, 46.3; H, 5.1%. IR ν_{max}/cm^{-1} 310s, br (Pt–Cl); 284vs, (Cu–Cl). MS (L-SIMS): *m*/*z* 998 ($M^+ - 2Cl$, 6%); 900 ($M^+ - Cu - 2Cl$, 75%). Λ(DMF) = 26.7 $ohm^{-1}\,cm^2\,mol^{-1}$. (**6b**) · $4H_2O$: Yield: 94%, green solid, m.p. 148 °C. $C_{42}H_{50}P_4PdCu_2Cl_4O_2$ requires: C, 45.1; H, 4.5. Found: C, 44.8; H, 4.4%. IR ν_{max}/cm^{-1} 310vs, br (Pd–Cl); 410m ν_a(Cu–Cl); 296s ν_s(Cu–Cl). Λ(DMF) = 82.5 $ohm^{-1}\,cm^2\,mol^{-1}$. (**7b**) · $4H_2O$ · $0.5CHCl_3$: Yield: 94%, green solid, m.p. 148 °C. $C_{42.5}H_{50.5}P_4PdCu_2Cl_{5.5}O_2$ requires: C, 45.1; H, 4.5. Found: C, 44.8; H, 4.4%. IR ν_{max}/cm^{-1} 310m, br (Pt–Cl); 296s ν_s(Cu–Cl). IR δ/cm^{-1} 110vs ($CuCl_2$). Λ(DMF) = 75.8 $ohm^{-1}\,cm^2\,mol^{-1}$.

2.3. *Titrations of **4** and **6a** with CuCl*

To a solution of complex **4** in CD_3OD or **6a** in $CDCl_3$, CuCl was added as a solid, reaching different stoichiometric ratios. The mixtures were stirred for 12 h, then DMSO-d_6 was added to solve the new complex formed and the $^{31}P\{^1H\}$ NMR spectra were recorded. The most significant signals are given in Table 1.

Table 1
$^{31}P\{^1H\}$ NMR data (r.t.) for complexes **1**–**7**, **1a**–**7a**, **6b** and **7b** and for reaction of **4** and **6a** with CuCl

Compound	δP^a	$^1J(^{31}P, ^{195}Pt)$	Solvent
1	34.6 s		$CDCl_3$
2[b]	109.4 t [1P], 44.3 d [2P]		$CDCl_3$
3	83.3 s [1P], 39.8 [2P]	3010, 2490	$CDCl_3$
4	37.7 br [1P], 34.1 br [1P], 23.6 s [1P]		CD_3OD
5	33.9 br [2P], −2.5 br [1P]	2738, 3317	CD_3OD
6	134.1 s [1P], 29.5 s [3P]		$CDCl_3$
7[c]	118.3 s [1P], 25.0 s [3P]	2505, 2590	$CDCl_3$
1a	37.0 br		$CDCl_3$
2a[b]	108.5 t [1P], 44.5 d [2P]		$CDCl_3$
3a[c]	83.4 s [1P], 39.7 s [2P]	3046, 2472	$CDCl_3$
4 + 1 eq. CuCl	35.7 br, −6.1br, −13.2 br		CD_3OD/DMSO-d_6
4a	36.9 br [2P], −11.1 br [1P]		DMSO-d_6
5a	34.9 br [2P], −0.9 s [1P]	2718, 3289	CD_3OD
6a	113.5 s [1P], 43.0 br [3P]		$CDCl_3$
7a	88.3 br [1P], 39.6 s [2P]*, 31.0 br [1P]	2496*	$CDCl_3$
6a + 1 eq. CuCl[b]	113.9 d [1P], 44.0 s [2P], 29.0 br [1P]		$CDCl_3$/DMSO-d_6
6b	121.5 s [1P], 49.9 s [2P], 33.7 br [1P]		DMSO-d_6
7b[b,c]	95.3 d [1P], 46.4 s [2P], 33.5 br [1P]	2957, 2507	DMSO-d_6

[a] Relative intensities: [nP].

[b] $^2J(^{31}P, ^{31}P)$: 9.4 Hz (**2**) (d,t); 9.5 Hz (**2a**) (d,t); 38.0 Hz (**6a** + 1 eq. CuCl) (d); 42.0 Hz (**7b**) (d).

[c] Compound (solvent), $\delta^{195}Pt/^1J(^{31}P, ^{195}Pt)$: **7** ($CDCl_3$), −4373dq/2590 Hz. **3a** ($CDCl_3$), −4875dt/3046, 2472 Hz. **7b** (DMSO-d_6), −4830dt/2947, 2520 Hz.

2.4. X-ray structure determination

A yellow crystal of **3a** was mounted on a glass fibre and used for data collection. Cell constants and an orientation matrix for data collection were obtained by least-squares refinement of the diffraction data from 25 reflections in the range of $10.497° < \theta < 18.002°$ in a ENRAF-NONIUS MACH 3 automatic diffractometer [18]. Data were collected at 293 K using Mo Kα radiation ($\lambda = 0.71073$ Å) and the ω scan technique and corrected for Lorentz and polarisation effects [19] and semi-empirical absorption correction (ψ scan) was made [20].

The structure was solved by direct methods [21], which revealed the position of all non-hydrogen atoms, and refined on F^2 by a full-matrix least-squares procedure using anisotropic displacement parameters [22]. The hydrogen atoms were located in their calculated positions (C–H 0.93–0.97 Å) and refined using a riding model. Atomic scattering factors from *International Tables for X-ray Crystallography* [23]. Molecular graphics from *ORTEP-3 for Windows* [24].

3. Results and discussion

3.1. Characterisation of complexes **1**–**7**

The conductivity measurements for 10^{-3} M DMF solutions of complexes **2**–**3**, **6** and **7** and a CH_3CN solution of **4** reveal that these systems behave as 1:1 electrolytes. However, complexes **1** and **5** exhibit molar conductivities in DMF (22.8 and 39.8 ohm^{-1} cm^2 mol^{-1}, respectively) that are lower than those expected in this solvent for 1:1 electrolytes (65–90 ohm^{-1} cm^2 mol^{-1}) [25], suggesting the presence of mixtures of species [16] or ionic pairs formation [17].

The FAB (**1**–**5**) and L-SIMS (**6**–**7**) mass spectra show in all cases peaks due to MLCl (L = polyphosphine ligand) fragments by loss of the Cl^- counter anion. For the NP_3 derivatives **4** and **5**, peaks assigned to oxidations of dangling P atoms of the ligand, $M(N(PO)P_2)Cl$ and $M(N(PO)_2P)Cl$, were also observed.

The $^{31}P\{^1H\}$ NMR spectrum of **1** (Table 1) shows one single resonance in consistence with PNHP acting as tridentate chelating ligand in a distorted square-planar arrangement to Pd(II) with the two equivalent P atoms mutually *trans* and the N atom *trans* to Cl. Likewise, the spectra for complexes **2** and **3** exhibit two resonances in a 1:2 integration ratio and support the formation of square-planar compounds where P_3 coordinates to M(II) through the three P atoms giving rise to two fused five-membered chelate rings. This is in agreement with $^1J(^{31}P, ^{195}Pt)$ couplings of 3010 and 2490 Hz for **3** typical of P *trans* to Cl and P *trans* to P, respectively [26,27].

The $^{31}P\{^1H\}$ NMR spectra for complexes **4** and **5**, containing the tripodal ligand NP_3, consist of three and two signals, respectively. The two signals at lower field for **4** exhibit a double integration ratio compared to the resonance at δ 23.6 and can be assigned to P atoms mutually *trans*. The broadening of these signals, corresponding to a 1:1 electrolyte, suggests the existence of an equilibrium between two five-coordinate species [15,28] with distorted square-pyramidal geometry at

Pd(II). The N and the P atom with the resonance at higher field can be alternating the *trans* to Cl and apical positions with all four donor atoms forming three fused five-membered rings (Scheme 1). The $^{1}J(^{31}P,^{195}Pt)$ coupling constants of 2738 and 3317 Hz obtained from the two broad peaks (in a 2:1 integration ratio) for **5** are in accordance with the presence of P *trans* to P and P *trans* to Cl, respectively [16]. The broadening decreased as the spectrum was recorded in CD_3OD above 40 °C, leading to a doublet and a triplet with $^{2}J(^{31}P,^{31}P)$ coupling constants of 20 Hz. The broadening of the signals below and at ambient temperature points to the existence of an equilibrium between a four-coordinate species whereby the metal is coordinated to one chloride and the three P atoms of the ligand forming three fused eight-membered chelate rings, and a five-coordinate species where the nitrogen is also coordinated to platinum (Scheme 1).

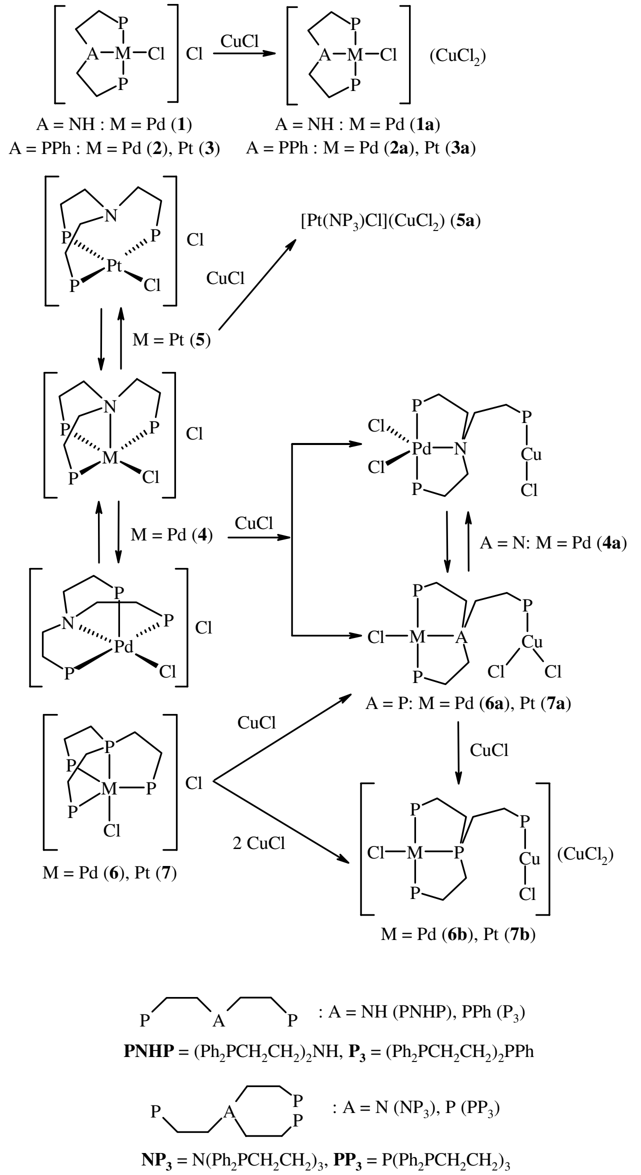

Scheme 1. Reactions with CuCl of the ionic complexes **1**–**3**, **5** to give the dichlorocuprate(I) derivatives **1a**–**3a**, **5a** and of the ionic precursors **4**, **6**–**7** to afford the neutral and ionic systems **4a**, **6a**–**7a** and **6b**–**7b**, respectively.

Complexes **6** and **7** containing the tripodal ligand PP_3 show a $^{31}P\{^{1}H\}$ NMR spectrum with two resonances in a 1:3 integration ratio (Table 1) supporting the formation of five-coordinate trigonal-bipyramidal systems [29,30] where the central P atom is in apical position *trans* to Cl and the three terminal P atoms are in the equatorial plane of the bipyramid (Scheme 1). This arrangement was confirmed for **7** from the $^{1}J(^{31}P,^{195}Pt)$ coupling values of 2505 and 2590 Hz characteristic of P *trans* to Cl and P in the equatorial plane, respectively. Likewise, the $^{195}Pt\{^{1}H\}$ NMR spectrum of **7** showed, as expected, an overlapped doublet of quartets at δ −4373 from which the $^{1}J(^{31}P,^{195}Pt)$ coupling of 2590 Hz was obtained.

The near far infrared spectrum of **1** showed a band at 3436 cm^{-1} assignable to the N–H vibration and shifted to higher energy compared to the band observed at 3300 cm^{-1} for the free amine, as a result of the complexation [17,31].

The far infrared spectra for **1**–**7** exhibit in all cases one band assigned to one terminal M–Cl bond in agreement with the other characterisation data.

3.2. Formation of mononuclear monocationic complexes with $CuCl_2^-$ as counter anion

The reaction of complexes **1**–**3** (containing linear ligands) and **5** (containing the tripodal ligand NP_3) with CuCl occurs without any chelate ring-opening giving compounds **1a**–**3a** and **5a** where $CuCl_2^-$ is the counter anion.

Complexes **2a** and **3a** were also obtained in lower yields (47% and 41% versus 90% and 79%) by interaction between the dinuclear complex, $Cu_2(\mu\text{-}P_3)_2Cl_2$ [32] and MCl_2 (M = Pd, Pt) in $CHCl_3$ using the same Cu:M ratio (Eq. (1)).

$$Cu_2(\mu\text{-}P_3)_2Cl_2 + 2MCl_2 \rightarrow \underset{\mathbf{2a},\ \mathbf{3a}}{2[M(P_3)Cl](CuCl_2)} \qquad (1)$$

The P_3 derivatives **2a** and **3a** behave as 1:1 electrolytes in 10^{-3} M DMF solutions. However, 10^{-3} M CH_3CN solutions of the PNHP derivative **1a** are not conductors in consistence with ion pairs formation [17].

The FAB mass spectra for **1a**–**3a** and **5a** show peaks assignable in all cases to MLCl (M = Pd, Pt, L = PNHP, P_3, NP_3) fragments.

The $^{31}P\{^{1}H\}$ NMR spectrum of **1a** in $CDCl_3$ shows one resonance at δ 37.0 slightly shifted to lower field compared to **1**. This resonance is assigned to the two equivalent phosphorus of the tridentate ligand mutually *trans*. For **2a** and **3a**, the spectra show two signals with integration ratio 1:2 from lower to higher field attributed to P *trans* to Cl and P mutually *trans*, respectively. The $^{1}J(^{31}P, ^{195}Pt)$ couplings for **3a** of 3046 and 2472 Hz confirm a retention of the distorted square-planar arrangement of the precursor and are coincident with the couplings obtained from the $^{195}Pt\{^{1}H\}$ NMR spectrum that consists of a doublet of triplets centred at δ −4875.

The $^{31}P\{^{1}H\}$ NMR spectrum of **5a** shows two signals at δ 34.9 and −0.9 in a 2:1 integration ratio, respectively, the $^{1}J(^{31}P, ^{195}Pt)$ coupling constants of 2718 and 3289 Hz being characteristic of P *trans* to P and P *trans* to Cl, respectively, as also found for the precursor.

As occurred for **1**, complex **1a** shows a N–H vibration in the near infrared spectrum at higher energy (3446 cm^{-1}) than the stretching mode found for the free amine (3300 cm^{-1}) as a consequence of complexation [16].

The far infrared spectra of **1a**–**3a** and **5a** are consistent with the presence of terminal M–Cl bonds and $CuCl_2^-$ anions. The bands at 396, 404, 400 and 390 cm^{-1} correspond to the asymmetric ν(Cu–X) stretching mode of the bent ClCuCl units and the bands at 296 and 282 cm^{-1} for (**1a**, **5a**) and (**2a**, **3a**), respectively, were due to the symmetric ν(Cu–X) mode. In addition, the bands at 109, 115 and 117 cm^{-1} for **1a**, (**2a**, **5a**) and **3a**, respectively, were attributed to the $\delta(CuCl_2)$ bending vibration [33].

It should be noted that the reactivity of complexes **1**–**3** and **5** with monovalent group 11 cations is influenced by the polyphosphine ligand and both the d^8 and d^{10} metal ions. Thus, while the reaction with CuCl, here reported, gives in all four cases the dichlorocuprate(I) derivatives and the reaction of $AgNO_3$ with **1**–**3** leads to the formation of the nitrate compounds, $[M(L)(ONO_2)](NO_3)$ (L = PNHP, M = Pd; L = P_3, M = Pd, Pt) [13,17], the addition of $AgNO_3$ to complex **5** does not allow the isolation of any complex [15b]. On the other hand, Au(tdg)Cl (tdg = thiodiglycol) produces abstraction of PNHP from **1** giving the dinuclear compound $Au_2(PNHP)Cl_2$ [17] and reacts with **2**–**3** via a ring-opening process with formation of the heterobimetallic systems $MAu(P_3)Cl_3$ [12]. No heterobimetallic compound was isolated by interaction of **5** with Au(tdg)Cl [15a].

3.3. Crystallography of **3a**

Recrystallisation of **3a** in acetone/ether solutions afforded single crystals of the entitled compound.

A perspective view of the molecular structure and numbering scheme is shown in Fig. 1. A summary of crystal parameters, data collection and refinement for this crystal structure is given in Table 2 and selected bond lengths and angles are listed in Table 3.

The complex consists of a monocation with a distorted square-planar geometry for platinum and a dichlorocuprate(I) anion with a slightly distorted linear ClCuCl arrangement.

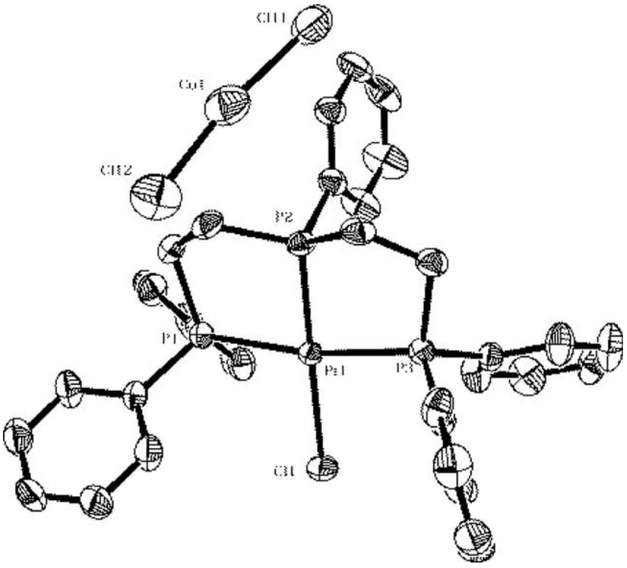

Fig. 1. Crystal structure of **3a**.

Table 2
Summary of crystal parameters, data collection and refinement for **3a**

Complex	**3a**
Empirical formula	$C_{34}H_{33}Cl_3CuP_3Pt$
Formula weight	899.49
Temperature (K)	293(2)
Wavelength (Å)	0.71073
Crystal size (mm)	0.20 × 0.20 × 0.20
Colour/habit	yellow/prisms
Crystal system	monoclinic
Space group	$P2_1/n$
a (Å)	10.1244(9)
b (Å)	20.1633(15)
c (Å)	16.6257(11)
α (°)	90
β (°)	93.782(6)
γ (°)	90
Volume ($Å^3$)	3386.6(5)
Z	4
Calculated density (Mg/m^3)	1.764
Absorption coefficient (mm^{-1})	5.156
$F(000)$	1760
θ range for data collection (°)	2.25–26.29
Index ranges	$-12 \leqslant h \leqslant 12$, $0 \leqslant k \leqslant 25$, $0 \leqslant l \leqslant 20$
Reflections collected	7112
Independent reflections	6875 [R_{int} = 0.0335]
Maximum and minimum transmission	0.985 and 0.876
Data/restraints/parameters	6875/0/ 379
Goodness of fit on F^2	0.984
Final R indices	$R_1 = 0.0316$, $w_2R = 0.0606$
Largest differential peak and hole (e $Å^{-3}$)	0.928 and −0.840

The Pt–P bond lengths in the monocation of 2.320 (P1), 2.207 (P2) and 2.310 (P3) Å are in the expected range and almost coincident with the same distances for the precursor complex **3** [12], with the Pt–P(2) bond

Table 3
Selected distances (Å) and angles (°) for **3a**

Complex	**3a**
Pt(1)–P(1)	2.320(2)
Pt(1)–P(2)	2.207(2)
Pt(1)–P(3)	2.310(2)
Pt(1)–Cl(1)	2.349(2)
Cu(1)–Cl(11)	2.103(2)
Cu(1)–Cl(12)	2.091(2)
P(1)–Pt(1)–P(2)	84.33(5)
P(1)–Pt(1)–P(3)	169.39(5)
P(2)–Pt(1)–P(3)	85.07(5)
P(1)–Pt(1)–Cl(1)	97.64(5)
P(2)–Pt(1)–Cl(1)	176.81(5)
P(3)–Pt(1)–Cl(1)	92.93(5)
Cl(11)–Cu(1)–Cl(12)	170.43(9)

being shorter than the Pt–$P_{terminal}$ due to the double chelate effect. The Pt–Cl distance of 2.349 Å is within the expected values for a terminal bond. The PPtP angles, 85.07°, 84.3°, and PPtCl, 176.81°, 169.39°, 97.64°, and 92.93°, confirm the distorted square-planar geometry at Pt(II). The coordination sphere for Pt(1) is tetrahedrally distorted from planar arrangement, with the two mutually *trans* P atoms [P(1) and P(3)] on one side (0.017 and 0.018 Å) of the least-squares plane defined by [P(1)P(2)P(3)Cl(1)] and with the central phosphorus and the chlorine (0.019 and 0.015 Å) atoms on the opposite side. The platinum atom was deviated 0.032 Å from the least-squares plane and to the same side as the phosphorus P(1) and P(3).

There were not found unusual inter or intracationic contacts. The $CuCl_2^-$ anions show CuCl bond lengths of 2.091 and 2.103 Å shorter than the same distances for other chlorocuprates(I) such as $[CuCl_3]^{2-}$ (av. 2.22 Å) [34] and $[Cu(PPh_3)Cl_2]^-$ (av. 2.24 Å) [33] or for the neutral compound $[Cu(PPh_3)_2Cl]$ (2.21 Å) [35]. The ClCuCl angle of 170.4° indicates a distortion (about 10°) from the ideal linear geometry. Concerning interanionic interactions, there is a Cu–Cl distance of 3.317 Å that involves Cu(1) and the chlorine atom of an adjacent $CuCl_2^-$ anion. This produces an intermetallic separation of 3.853 Å which is 0.425 Å longer than the Cu···Cu distance of 3.428 Å found in $[Cu_2(PPh_3)_2I_4]^{2-}$, where two three-coordinate metal centres are bridged by two iodide anions [33]. There are not unusual cation–anion interactions with a separation between Pt(1) and Cu(1) of 6.136 Å.

3.4. Neutral heterobimetallic complexes obtained by ring-opening reaction

The precursors containing tripodal polyphosphine ligands $[Pd(NP_3)Cl]Cl$ (**4**) and $[M(PP_3)Cl]Cl$ [M = Pd (**6**), Pt (**7**)] react with one equivalent of CuCl to give the heterobimetallic systems $PdCu(NP_3)Cl_3$ (**4a**) and $MCu(PP_3)Cl_3$ [M = Pd (**6a**), Pt (**7a**)].

Fig. 2 shows the titration of **4** with CuCl followed by $^{31}P\{^1H\}$ NMR. The addition of one equivalent of CuCl produces a slight shift to higher field of the resonance at δ 37.7 and the disappearance of the signals at δ 34.1 and 23.6 of the precursor (Fig. 2(a)). The resultant spectrum (Fig. 2(b)) exhibits three resonances at δ 35.7, −6.1 and −13.2 pointing to the formation of two isomers for **4a**. The most intense resonance at lower field can be assigned to P atoms mutually *trans* bound to Pd(II) in two environments with the ligand adopting the same coordination mode, and the two broad signals at higher field can be attributed to P atoms bound to Cu(I) that achieves two different coordination numbers. The $^{31}P\{^1H\}$ NMR spectrum for solutions of **4a** in DMSO-d_6 shows two broad resonances at δ 36.9 and −11.1 with the signal at higher field, due to P bound to Cu(I), including the two signals found in the titration. Addition of a second equivalent of CuCl to **4** does not produce any modification (Fig. 2(c)). Since solutions of **4a** in CH_3CN behave as non-conductors, two neutral structures are proposed. One contains trigonal-bipyramidal (Cl_2PdNP_2) and linear (PCuCl) arrangements and the other distorted square-planar ($ClPdNP_2$) and trigonal planar ($PCuCl_2$) geometries for Pd(II) and Cu(I), respectively (Scheme 1). Thus, one of the three fused five-membered rings of **4** is opened by interaction with CuCl, the phosphine acting as tridentate chelating for Pd(II) and monodentate bridging ligand for Cu(I). On the basis of the broadening of the peaks, another neutral form with NP_3 acting as bidentate ligand to palladium (Cl_2PdNP) and copper (P_2CuCl) should not be excluded.

The presence of a peak in the FAB mass spectrum of **4a** due to $PdCu(NP_3)Cl_2$ confirms the formation of heteronuclear species. Furthermore, another peak with 0.5% abundance was observed at *m*/*e* = 1819 attributable to a $Pd_2Cu_2(NP_3)_2Cl_5$ fragment. This coexistence in some extent of heterodinuclear and heterotetranuclear structures was also observed for the analogous system $PdAg(NP_3)Cl_3$ [15b].

The two bands at 337 and 255 cm^{-1} found in the far infrared spectrum of **4a** are consistent with the existence of terminal Pd–Cl and Cu–Cl bonds, respectively.

The trigonal-bipyramidal arrangements for M(II) in **6** and **7** change to distorted square-planar in complexes **6a** and **7a** upon reaction with one equivalent of CuCl. The resultant compounds behave as non-conductors in 10^{-3} M DMF solutions showing peaks in their L-SIMS mass spectra due to $MCu(PP_3)Cl$ and $M_2Cu_2(PP_3)_2Cl_5$ [*m*/*e* = 1853 (M = Pd, 1%), 2031 (M = Pt, 1%)] fragments. The $^{31}P\{^1H\}$ NMR spectra show two and three resonances for **6a** (Fig. 3(a)) and **7a**, respectively, with the broad signal at higher field for **6a** (δ 43.0) including the two signals (δ 39.6, 31.0) found for **7a**. The peak of **7a** at lower field was assigned to the central P atom *trans* to Cl, the resonance in the middle to two P atoms

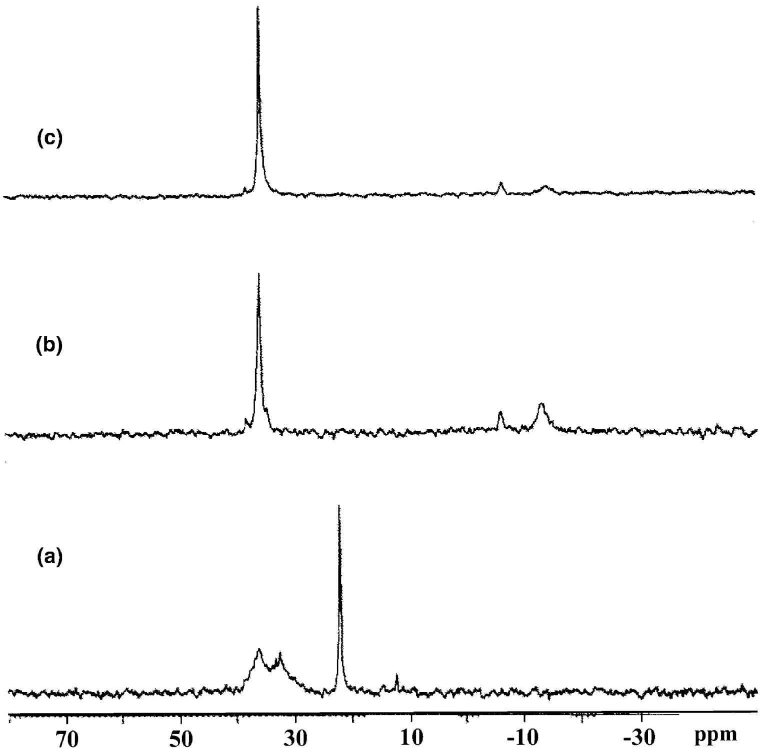

Fig. 2. $^{31}P\{^1H\}$ NMR spectra in $CD_3OD/DMSO\text{-}d_6$ of (a) complex **4**, (b) **4** + 1 mol eq. of CuCl affording complex **4a** and (c) **4a** + 1 mol eq. of CuCl.

mutually *trans* and the signal at higher field to one P atom bound to one $CuCl_2$ moiety. The $^1J(^{31}P, ^{195}Pt)$ coupling constant of 2496 Hz obtained from the resonance at δ 39.6 confirms the presence of P *trans* to P. These data point to the formation of complexes containing distorted square-planar M(II) and trigonal planar Cu(I) centres as it was proposed for one of the isomers of **4a** (Scheme 1).

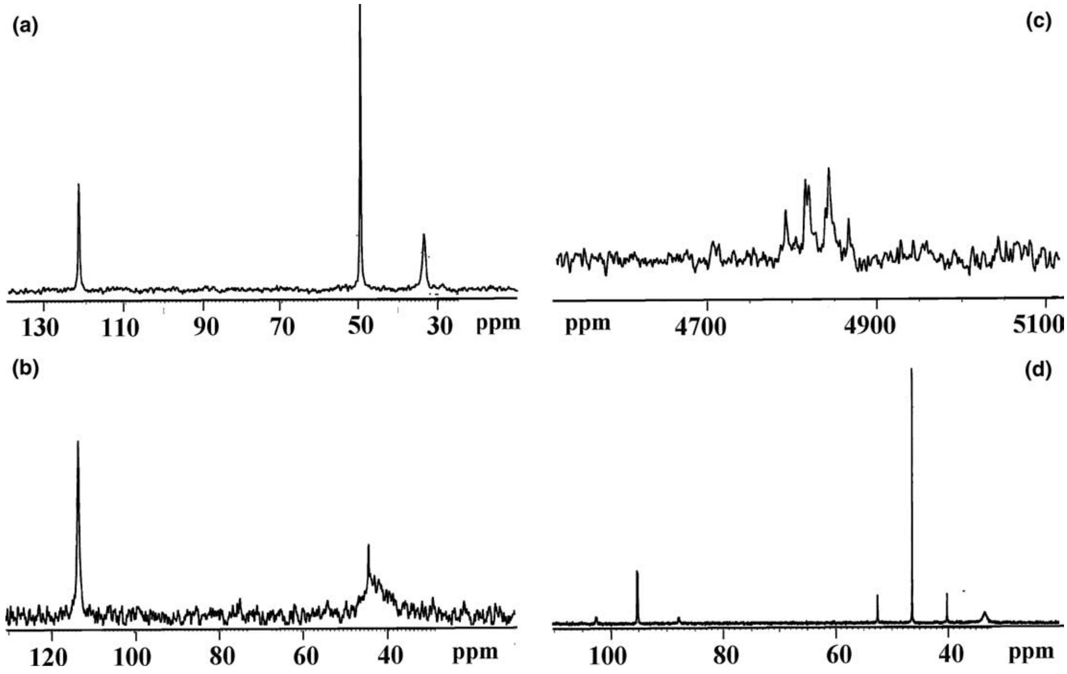

Fig. 3. $^{31}P\{^1H\}$ NMR spectra for: (a) $PdCu(PP_3)Cl_3$ (**6a** in $CDCl_3$), (b) $[PdCu(PP_3)Cl_2](CuCl_2)$ (**6b** in $DMSO\text{-}d_6$), (c) $[PtCu(PP_3)Cl_2](CuCl_2)$ (**7b** in $DMSO\text{-}d_6$). (d) $^{195}Pt\{^1H\}$ NMR spectrum for **7b** in $DMSO\text{-}d_6$.

The bands in the far infrared spectrum at 300, 285 and 310, 284 cm^{-1} for **6a** and **7a** were attributed to terminal M–Cl and Cu–Cl bonds, respectively, with the broadening of the vibration at higher energy suggesting the inclusion of *v*(M–Cl) and *v*(Cu–Cl).

It should be noted that the precursors **4**, **6** and **7**, containing tripodal ligands, form heterobimetallic compounds not only by reaction with CuCl but also with Au(tdg)Cl ($\mathrm{MAu(NP_3)Cl_3}$, $\mathrm{[MAu(PP_3)Cl_2]Cl}$), AgCl or $\mathrm{AgNO_3}$ [15].

3.5. Formation of monocationic heterobimetallic complexes with $\mathrm{CuCl_2}^-$ as counter anion

When complexes **6** and **7** react with two equivalents of CuCl, the heterobimetallic monocationic compounds **6b** and **7b**, respectively, containing one $\mathrm{CuCl_2}^-$ counter anion were formed. These compounds were also afforded by interaction of **6a** and **7a** with one equivalent of CuCl, demonstrating that only the first equivalent of CuCl added to **6** and **7** is involved in a ring-opening process with the second one changing the ionicity of the resultant heterobimetallic systems. Indeed, the molar conductivities for 10^{-3} M DMF solutions of **6b** and **7b** reveal an ionogenic behaviour corresponding to 1:1 electrolytes, while compounds **6a** and **7a** were shown to be non-conductors in the same solvent (vide supra).

The L-SIMS mass spectra for both complexes show a peak with 100% abundance attributed to $\mathrm{M(P(PO)P_2)Cl}$ fragments, which is consistent with the loss of the CuCl moiety from the cations $\mathrm{[MCu(PP_3)Cl_2]^+}$ and oxidation of the dangling phosphorus. No peak assigned to heterotetrametallic species (as observed for **6a** and **7a**) was detected now.

The $^{31}\mathrm{P}\{^1\mathrm{H}\}$ NMR spectra show three signals [Fig. 3(b) (**6b**), Fig. 3(c) (**7b**)] with a 1:2:1 integration ratio supporting the presence of two types of P atoms bound to M(II) and one third bound to Cu(I) (Scheme 1). The signals at lower field for **7b** allow the $^1J(^{31}\mathrm{P}, ^{195}\mathrm{Pt})$ couplings of 2957 and 2507 Hz in accordance with P *trans* to Cl and P *trans* to P, respectively. Similar coupling constants were obtained from the $^{195}\mathrm{Pt}\{^1\mathrm{H}\}$ NMR spectrum in DMSO-$\mathrm{d_6}$, which consisted of an overlapped doublet of triplets at −4830 (Fig. 2d) corresponding to a distorted square-planar arrangement to Pt(II), $\mathrm{ClPtP_3}$ [12]. As also observed for $\mathrm{[PtAu(PP_3)Cl_2]Cl}$ [15a], this resonance appears higher field shifted compared to the overlapped doublet of quartets at δ −4373 ($\mathrm{CDCl_3}$) found for the trigonal-bipyramidal precursor **7** [30].

The broad bands in the far infrared spectra at 310 cm^{-1} for **6b** and **7b** are consistent with the presence of terminal M–Cl and Cu–Cl bonds in the cationic complexes. On the other hand, the appearance of vibrations assigned to copper-chloride stretching (**6b**, **7b**) and bending (**7b**) modes evidences the existence of dichloro cuprate(I) anions [36].

It should be noted that while excess CuCl and AgCl [15b] only produce a ring-opening from the precursors **4**, **6** and **7** to give compounds $\mathrm{MM'(L)Cl_3}$ [L = $\mathrm{NP_3}$, M = Pd, M′ = Cu, Ag; L = $\mathrm{PP_3}$, M = Pd, Pt, M′ = Cu, Ag] and $\mathrm{[MCu(PP_3)Cl_2](CuCl_2)}$ (M = Pd, Pt), the addition of Au(tdg)Cl to the heterobimetallic systems $\mathrm{[MAu(PP_3)Cl_2]Cl}$ (M = Pd, Pt) results in a second ring-opening with formation of $\mathrm{MAu_2(PP_3)Cl_4}$ [15a].

4. Conclusions

CuCl reacts with distorted square-planar complexes containing linear polyphosphines of the type [M(L)Cl]Cl (L = PNHP, M = Pd; L = $\mathrm{P_3}$, M = Pd, Pt) to give the corresponding dichlorocuprates(I). The crystal structure of $\mathrm{[Pt(P_3)Cl](CuCl_2)}$ consists of monocations, where Pt(II) retains the distorted square-planar arrangement, and $\mathrm{CuCl_2}^-$ anions with a certain distortion from the linear geometry. However, the reaction of $\mathrm{[M(NP_3)Cl]Cl}$ with CuCl affords a heterobimetallic complex when M = Pd and the dichlorocuprate(I) derivative when M = Pt. On the other hand, the trigonal-bipyramidal complexes $\mathrm{[M(PP_3)Cl]Cl}$ (M = Pd, Pt) containing a tripodal tetraphosphine react with one and two equivalents of CuCl to give heterobimetallic neutral $\mathrm{MCu(PP_3)Cl_3}$ and ionic $\mathrm{[MCu(PP_3)Cl_2](CuCl_2)}$ compounds, respectively, via a ring-opening process.

5. Supplementary material

A complete set of X-ray crystallographic structural studies for complex **3a** (CCDC No. 230211) is available at the Cambridge Crystallographic Data Centre, 12 Union Road, Cambridge CB2 1EZ, UK (fax: +44 1223 336 033; e-mail: deposit@ccdc.cam.ac.uk) on request, quoting the deposition number.

Acknowledgements

We thank Xunta de Galicia for financial support. Crystallographic data for complex **3a** were measured at the Unidade de Raios X, RIAIDT, University of Santiago de Compostela, Spain.

References

[1] (a) N. Wheatly, P. Kalck, Chem. Rev. 99 (1999) 3379;
(b) D.W. Stephan, T.T. Nadasdi, Coord. Chem. Rev. 147 (1996) 147;
(c) R.M. Bullock, C.P. Casey, Acc. Chem. Res. 20 (1987) 167;
(d) D.W. Stephan, Coord. Chem. Rev. 95 (1989) 41;

(e) R.D. Adams, in: G. Wilkinson, F.G.A. Stone, E.W. Abel (Eds.), Comprehensive Organometallic Chemistry, vol. 10, Pergamon, Oxford, UK, 1995, p. 1.

[2] (a) N. Feikeu, P. Pregosin, G. Trabesinger, Organometallics 17 (1998) 4510;
(b) J.M. Rosset, M.P. Glenn, J.D. Cotton, A.C. Willis, C.H.L. Kennard, K.A. Bryiel, B.H. Riches, W. Kitching, Organometallics 17 (1998) 1968.

[3] (a) J.W. Steed, D.A. Tocher, Inorg. Chim. Acta 229 (1995) 87;
(b) K. Severin, K. Polborn, W. Beck, Inorg. Chim. Acta 240 (1995) 339;
(c) K. Heinze, G. Huttner, L. Zsolnai, P. Schober, Inorg. Chem. 36 (1997) 5457;
(d) K. Polborn, K. Severin, Eur. J. Inorg. Chem. (1998) 1187;
(e) J.J. Vittal, P.A.W. Dean, Polyhedron 17 (1998) 1937;
(f) M. Öhm, A. Schulz, K. Severin, Eur. J. Inorg. Chem. (2000) 2623.

[4] (a) I. Ara, J.R. Berenguer, E. Equizábal, J. Forniés, E. Lalinde, A. Martín, F. Martínez, Organometallics 17 (1998) 4578;
(b) I. Ara, J.R. Berenguer, E. Equizábal, J. Forniés, E. Lalinde, A. Martín, Eur. J. Inorg. Chem. (2001) 1631;
(c) J. Forniés-Cámer, A.M. Masdeu-Bultó, C. Claver, Organometallics 21 (2002) 2609.

[5] G.J. Matare, M.E. Tess, Y. Yang, K.A. Abboud, L. McElwee-White, Organometallics 21 (2002) 711.

[6] B. Bosnich, Inorg. Chem. 38 (1999) 2554.

[7] S.E. Watkins, D.C. Craig, S.B. Colbran, J. Chem. Soc., Dalton Trans. (2002) 2423.

[8] (a) H.K. Yip, C.M. Che, S.M. Peng, Chem. Commun. 22 (1991) 1626;
(b) C.-M. Che, M.-C. Tse, M.C.W. Chan, K.-K. Cheung, D.L. Phillips, K.-H. Leung, J. Am. Chem. Soc. 122 (2000) 2464;
(c) H.K. Yip, H.M. Lin, Y. Wang, C.M. Che, J. Chem. Soc., Dalton Trans. (1993) 2939;
(d) H.K. Yip, H.M. Lin, Y. Wang, C.M. Che, Inorg. Chem. 32 (1993) 3402.

[9] C.-M. Che, B.-H. Xia, J.-S. Huang, C.-K. Chan, Z.-Y. Zhou, K.-K. Cheung, Chem. A: Eur. J. 7 (2001) 3998.

[10] (a) S.W. Carr, P.G. Pringle, B.L. Shaw, J. Organomet. Chem. 341 (1988) 543;
(b) P. Braunstein, J. Durand, X. Morise, A. Tiripicchio, F. Ugozzoli, Organometallics 19 (2000) 444;
(c) J. Blin, P. Braunstein, J. Fisher, G. Kickelbick, M. Knorr, X. Morise, T. Wirth, Inorg. Chem. 13 (1999) 2159.

[11] T. Tanase, H. Toda, Y. Yamamoto, Inorg. Chem. 36 (1997) 1571.

[12] P. Sevillano, A. Habtemariam, S. Parsons, A. Castiñeiras, M.E. García, P.J. Sadler, J. Chem. Soc., Dalton Trans. (1999) 2861.

[13] D. Fernández, P. Sevillano, M.I. García-Seijo, A. Castiñeiras, L. Jánosi, Z. Berente, L. Kollár, M.E. García-Fernández, Inorg. Chim. Acta 312 (2001) 40.

[14] M.I. García-Seijo, A. Habtemariam, D. Fernández, S. Parsons, M.E. García-Fernández, Z. Anorg. Allg. Chem. 628 (2002) 1075.

[15] (a) D. Fernández, M.I. García-Seijo, A. Castiñeiras, M.E. García-Fernández, Dalton Trans. (2004) 2526;
(b) D. Fernández, M.I. García-Seijo, A. Castiñeiras, M.E. García-Fernández, 10ª Reunión Científica Plenaria de Química Inorgánica, Córdoba, Spain, 2002, p. 22 (abstract).

[16] M.I. García-Seijo, A. Habtemariam, P. del S. Murdoch, R.O. Gould, M.E. García-Fernández, Inorg. Chim. Acta 335 (2002) 52.

[17] M.I. García-Seijo, A. Habtemariam, S. Parsons, R.O. Gould, M.E. García-Fernández, New J. Chem. 26 (2002) 636.

[18] Enraf-Nonius, CAD4-Express Software. Version 5.1. Enraf-Nonius, Delft, The Netherlans, 1995.

[19] A.L. Spek, HELENA. A Program for Data Reduction of CAD4 Data, University of Utrecht, The Netherlands, 1997.

[20] A.L. Spek, PLATON. A Multipurpose Crystallographic Tool, University of Utrecht, The Netherlands, 1997.

[21] G.M. Sheldrick, Acta Crystallogr. A46 (1990) 467.

[22] G.M. Sheldrick, SHELXL-97. Program for Refinement of Crystal Structures, University of Goettingen, Germany, 1997.

[23] International Tables for X-ray Crystallography, vol. C, Kluwer Academic Publishers, Dordrecht, The Netherlands, 1995.

[24] L.J. Farrugia, J. Appl. Crystallogr. 30 (1997) 565.

[25] W.J. Geary, Coord. Chem. Rev. 7 (1971) 81.

[26] A. Handler, P. Peringer, J. Chem. Soc., Dalton Trans. (1990) 3725.

[27] G.K. Anderson, H.C. Clark, J.A. Davies, Inorg. Chem. 83 (1983) 434.

[28] M.M. Taqui Khan, E. Rama Rao, Polyhedron 7 (1988) 29.

[29] S. Aizawa, T. Iida, S. Funahashi, Inorg. Chem. 35 (1996) 5163.

[30] D. Fernández, M.I. García-Seijo, T. Kégl, G. Petöcz, L. Kollár, M.E. García-Fernández, Inorg. Chem. 47 (2002) 4435.

[31] (a) R.M. Silverstein, G.C. Bassler, T.C. Morril, Spectrometric identification of organic compounds, fourth ed., John Wiley & Sons, New York, 1981;
(b) L.M. Harwood, C.J. Moodly, J.M. Percy, Experimental Organic Chemistry, second ed., Blackwell Science Ltd., UK, 1999.

[32] R.D. Hart, B.W. Skelton, A.H. White, Aust. J. Chem. 44 (1991) 919.

[33] G.A. Bowmaker, W. Jirong, R.D. Hart, A.H. White, P.C. Healy, J. Chem. Soc., Dalton Trans. (1992) 787.

[34] S. Andersson, S. Jagner, Acta Chem. Scand., Ser. A 42 (1988) 691.

[35] G.A. Bowmaker, J.C. Dyason, P.C. Healy, L.M. Engelhardt, C. Pakawatchai, A.H. White, J. Chem. Soc., Dalton Trans. (1987) 1089.

[36] D.N. Waters, B. Basak, J. Chem. Soc. A (1971) 2733.